

DIFFUSION-WAVE FLOOD ROUTING IN CHANNEL NETWORKS

By Ali Osman Akan¹ and Ben Chie Yen,² F. ASCE

INTRODUCTION

For subcritical flow in an open-channel network, mutual backwater effects exist among the channel branches joining at a junction. Therefore, the branches cannot be treated individually when a dynamic wave model (4,10) is adopted to route floods in an open-channel network. Ideally, the entire network should be considered as a single unit and the flow in all the channels and junctions should be solved simultaneously. However, for a network consisting of more than a few channels, this approach requires an excessive amount of computer storage and expense.

In the sequential type models (3,6) traditionally employed for routing floods through a channel network, the difficulty caused by the mutual backwater effect of channels does not arise because the backwater effect from downstream is ignored. The routing starts from the most upstream channels and is carried towards downstream, channel by channel in sequence, satisfying the flow continuity requirement at junctions. The downstream boundary condition of a channel required in the computations is treated somewhat casually since it actually is unknown at the time of seeking a solution. However, Sevük and the second writer (8), and the writers (11) have shown that sequential models give unrealistic solutions when the downstream backwater effect is significant.

In order to reduce the high computer cost and storage requirements in solving large network problems, a successive decomposition technique called the overlapping-segment scheme has been employed in routing floods through channel networks (7,11). An example is given in Fig. 1. Solution is sought separately and successively for each individual segment which consists of one junction and the channels joining it. Consequently, the computer storage requirement is substantially decreased. When the Saint Venant equations, together with the junction continuity and dynamic equations are employed to describe the flow, the coefficient matrix involved in the solution process is not banded and therefore the matrix solution technique is not most efficient.

¹Asst. Prof. of Civ. Engrg., Middle East Technical Univ., Ankara, Turkey.

²Prof. of Civ. Engrg., Univ. of Illinois at Urbana-Champaign, Urbana, Ill. 61801.

Note.—Discussion open until November 1, 1981. To extend the closing date one month, a written request must be filed with the Manager of Technical and Professional Publications, ASCE. Manuscript was submitted for review for possible publication on July 22, 1980. This paper is part of the Journal of the Hydraulics Division, Proceedings of the American Society of Civil Engineers, ©ASCE, Vol. 107, No. HY6, June, 1981. ISSN 0044-796X/81/0006-0719/\$01.00.

Another avenue to reduce the computational costs in flow routing is to use an approximation to the Saint-Venant equations (dynamic wave) instead of the complete equations. It is well-known that only approximations of the level of diffusion wave model or higher can account for the downstream backwater effect whereas the kinematic wave models cannot (10). Ponce, et al. (5) investigated the conditions under which the diffusion wave can be a good approximation of the dynamic wave model.

In this paper, a nonlinear diffusion wave model to simulate the unsteady flow in a dendritic network accounting for the downstream backwater effect is presented. The overlapping-segment technique is applied to the diffusion wave equations which are written in finite differences. The resulting set of nonlinear algebraic equations for each segment is solved by using the Newton iteration method. The coefficient matrices obtained in the solution process are banded and, therefore, the matrix equations are solved by a very efficient numerical

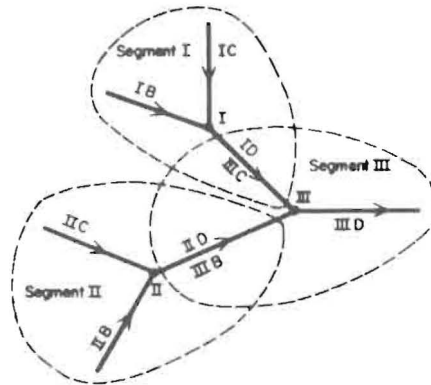


FIG. 1.—Overlapping Segments

technique. The results of the proposed model compare favorably to those of a complete dynamic wave and of a kinematic wave model.

UNSTEADY FLOW EQUATIONS

Gradually varied unsteady flow in open channels is mathematically described by a set of one-dimensional shallow water equations commonly known as the Saint-Venant equations. In a gravity-oriented coordinate system, these equations are written as (9,10)

$$\frac{\partial A}{\partial t} + \frac{\partial Q}{\partial x} = 0 \quad (1)$$

$$\frac{\partial Q}{\partial t} + \frac{\partial}{\partial x} \left(\beta \frac{Q^2}{A} \right) + gA \left(\frac{\partial h}{\partial x} + S_f \right) = 0 \quad (2)$$

in which x = distance measured horizontally along the channel; A = flow cross-sectional area measured normal to x ; Q = discharge through A ; h = water surface elevation measured vertically from a horizontal datum; β =

momentum correction coefficient; g = gravitational acceleration; S_f = friction slope; and t = time. For practical purposes, β is usually taken as unity. The friction slope S_f for turbulent flow can be estimated by using Manning's formula

$$S_f = \frac{n^2 Q |Q|}{K^2 A^2 R^{4/3}} \quad (3)$$

in which n = the Manning roughness factor; R = hydraulic radius; and the constant $K = 1$ for SI units and 1.486 for U.S. Customary units. Alternatively, other friction formulas such as Darcy-Weisbach's or Chezy's may also be used.

Hydraulic conditions at a junction may be described by the continuity equation

$$\sum Q_k = Q_o + \frac{ds}{dt} \quad (4)$$

and the dynamic equation

$$h_k + \frac{V_k^2}{2g} - H_k = h_o + \frac{V_o^2}{2g} \quad (5)$$

in which s = the storage within the junction; H = head loss through the junction; and V = flow velocity. The subscript k stands for any one of the in-flowing channels and o represents the out-flowing channel. Other symbols are as previously defined.

Junctions have small storage volumes in most open-channel networks for which the term ds/dt in Eq. 4 is negligible. Thus, one can write

$$\sum Q_k = Q_o \quad (6)$$

Also, when the flows in all the branches joining at a junction are subcritical, Eq. 5 can be approximated by a kinematic compatibility condition as

$$h_k = h_o \quad (7)$$

DESCRIPTION OF PROPOSED DIFFUSION-WAVE MODEL

Diffusion Wave Equations.—In the diffusion wave approximation of the Saint-Venant equations, the local and convective acceleration terms in the momentum equation (i.e., the first two terms in Eq. 2) are neglected (10). Thus, Eq. 2 is simplified as

$$S_f = - \frac{\partial h}{\partial x} \quad (8)$$

Combining Eqs. 3 and 8 yields

$$Q = \frac{K}{n} A R^{2/3} \frac{-\frac{\partial h}{\partial x}}{\left| \frac{\partial h}{\partial x} \right|^{1/2}} \quad (9)$$

which may account for flows in both positive and negative x directions.

Finite Difference Equations.—Consider a Y-segment shown in Fig. 2 as an example. At the Y-junction, *B* and *C* are the two incoming channels and *D* is the outflowing channel. These channels are subdivided by *M*, *L*, and *N* cross sections, respectively, for the branches *B*, *C*, and *D*, into *M* – 1, *L* – 1, and *N* – 1 computational reaches. Numerical solutions are sought at the flow cross sections. Although the reach length, Δx , is allowed to vary in the model, it is treated here as a constant for a channel for simplicity.

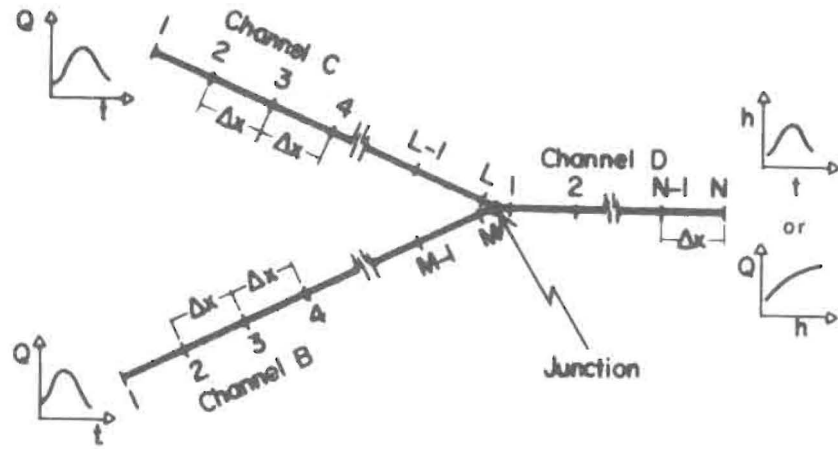


FIG. 2.—Discretization of a Y-Segment

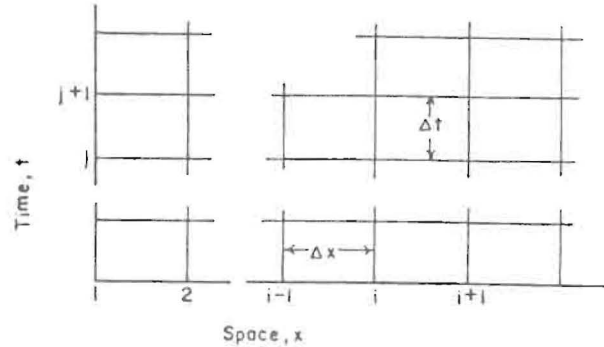


FIG. 3.—Computational Grid

Inflow discharge hydrographs at the upstream end of channels *B* and *C* are given as the upstream boundary conditions. In other words, $Q_{B,1}$ and $Q_{C,1}$ are prescribed functions of time where the first subscript denotes the channel and the second subscript stands for the flow section considered. A downstream boundary condition for channel *D* must also be known. This condition can be prescribed as a stage hydrograph or a stage-discharge relationship.

With reference to Fig. 3, Eq. 1 is written in finite difference quotients for a reach in Channel *B* as

$$\frac{A_{B,i+1}^{j+1} + A_{B,i}^{j+1} - A_{B,i+1}^j - A_{B,i}^j}{2\Delta t} + \frac{Q_{B,i+1}^{j+1} - Q_{B,i}^{j+1}}{\Delta x} = 0, \dots \quad (10)$$

in which $i = 1, 2, \dots, M - 1$. In Eq. 10, the superscript $j + 1$ = the time stage at which solutions are sought; and j = the previous time stage at which solutions are already known. The time increment between the two stages is denoted by Δt . The unknown terms in Eq. 10 are those containing the superscript $j + 1$ except for $Q_{B,1}^{j+1}$ which is specified as the upstream boundary condition. The discharge, Q , at an interior flow section is computed by using Eq. 9 which is written in finite difference form as

$$Q_{B,i+1}^{j+1} = \frac{K}{n_{B,i+1}} A_{B,i+1}^{j+1} (R_{B,i+1}^{j+1})^{2/3} \left| \frac{\frac{h_{B,i+1}^{j+1} - h_{B,i}^{j+1}}{\Delta x}}{\sqrt{\frac{h_{B,i+1}^{j+1} - h_{B,i}^{j+1}}{\Delta x}}} \right|^{1/2} \dots \quad (11)$$

Since the flow area A and the hydraulic radius R are known functions of the water surface elevation h , substituting Eq. 11 into Eq. 10 for $i = 1, 2, \dots, M - 1$, yields a set of $M - 1$ equations with M unknowns in the form of

$$f_{B,i}(h_{B,i-1}^{j+1}, h_{B,i}^{j+1}, h_{B,i+1}^{j+1}) = 0; \quad i = 1, 2, \dots, M - 1 \quad (12)$$

in which $h_{B,i}^{j+1}$ for $i = 1, 2, \dots, M$ are the unknowns.

Similarly, for channel *C*, a set of $L - 1$ equations with L unknowns are obtained as

$$f_{C,i}(h_{C,i-1}^{j+1}, h_{C,i}^{j+1}, h_{C,i+1}^{j+1}) = 0; \quad i = 1, 2, \dots, L - 1 \quad (13)$$

For channel *D* a set of $N - 2$ finite difference equations with N unknowns for the interior flow sections is

$$f_{D,i}(h_{D,i-1}^{j+1}, h_{D,i}^{j+1}, h_{D,i+1}^{j+1}) = 0; \quad i = 2, 3, \dots, N - 1 \quad (14)$$

The downstream boundary condition for channel *D* is expressed as

$$f_{D,N}(h_{D,N}^{j+1}) = 0 \quad (15)$$

Eqs. 12–15 together provide a total of $M + N + L - 3$ equations with $M + N + L$ unknowns. Additional three equations are obtained from the junction conditions. For the Y-junction being considered, Eq. 6 becomes

$$Q_{D,1}^{j+1} = Q_{B,M}^{j+1} + Q_{C,L}^{j+1} \quad (16)$$

Also, Eq. 7 written separately for branches *B* and *C* yields

$$h_{B,M}^{j+1} = h_{D,1}^{j+1} \quad (17)$$

$$h_{C,L}^{j+1} = h_{D,1}^{j+1} \quad (18)$$

Making use of Eq. 11 and the cross-sectional geometry of the channels, Eqs. 16–18 are expressed as

$$f_{D,1}(h_{D,1}^{j+1}, h_{B,M}^{j+1}, h_{C,L}^{j+1}) = 0 \quad (19)$$

$$f_{B,M}(h_{D,1}^{j+1}, h_{B,M}^{j+1}) = 0 \quad (20)$$

$$f_{C,L}(h_{D,1}^{j+1}, h_{C,L}^{j+1}) = 0 \quad (21)$$

FIG. 4.—Matrix Equation Solved in Each Iteration Cycle

HY6

Solution Technique for Finite Difference Equations.—The Newton iteration method is employed for the solution of the simultaneous nonlinear finite difference equations. The procedure can be summarized as follows:

1. A set of trial values, \hat{h}^{j+1} , are assigned to the unknowns h^{j+1} .
 2. Substituting \hat{h}^{j+1} into Eqs. 12–15 and Eqs. 19–21, \hat{f} values are computed.
 3. Partial derivatives of the functions f appearing in Eqs. 12–15 and Eqs. 19–21 with respect to h^{j+1} are taken and evaluated by using \hat{h}^{j+1} to yield $\partial\hat{f}/\partial h^{j+1}$.
 4. The matrix equation shown in Fig. 4 is obtained using the values of \hat{f} and $\partial\hat{f}/\partial h^{j+1}$. The superscripts $j + 1$ are not shown in Fig. 4 for the sake of clarity. It should be noted that the variables, $h_{B,M}^{j+1}$ and $h_{C,L}^{j+1}$, in Eq. 19, and the variable, $h_{D,1}^{j+1}$, in Eqs. 20 and 21 are treated as constants assuming their values as obtained at the previous iteration cycle while computing the partial derivatives of the functions $f_{D,1}$, $f_{B,M}$, and $f_{C,L}$. Only with this approximation can a banded coefficient matrix be obtained in Fig. 4.
 5. The matrix equation of Fig. 4 is solved for the corrections Δh . If the magnitudes of these corrections are within tolerable limits for all the flow sections,

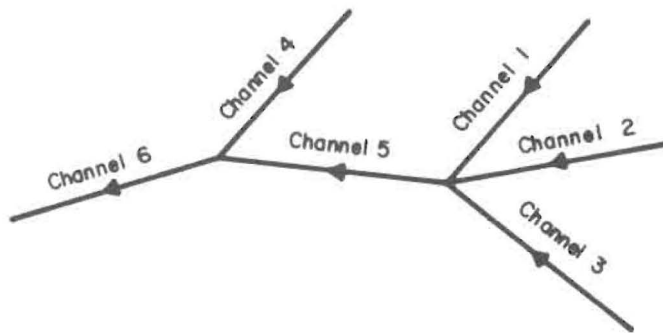


FIG. 5.—Hypothetical Network Used in Examples I and II

the trial values \hat{h} are accepted. Otherwise, the trial values are improved as $\hat{h} = \hat{h} + \Delta h$ for all the flow sections, and a new iteration cycle is initiated.

It should be noted that the coefficient matrix in Fig. 4 is banded with at most three nonzero elements on the diagonal. This allows a very efficient solution procedure which has been described elsewhere (1) in detail and will not be repeated here.

Overlapping-Segment Approach.—When flow in a channel network containing more than one junction is to be simulated, the proposed model employs an overlapping-segment technique as mentioned in the "Introduction." As shown in Fig. 1, the network is assumed to be composed of a number of segments each containing only one junction. The outflowing channel of a segment is also an inflowing channel of the immediate following segment. For instance, in Fig. 1 the out-flowing channel ID of segment I serves also as the inflowing channel IIIC for segment III.

Each segment is treated as a separate unit in the computation. Computations

start from upstream segments and progress towards downstream. For example, in Fig. 1, first, segments I and II are considered separately with the downstream boundary conditions for channels ID and IID assumed to be approaching the normal flow for a long channel. Finite difference equations for each of these two segments are obtained and solved respectively in a manner similar to those previously described for the simple Y-segment of Fig. 2. The only exception is that Eq. 15 is replaced by a uniform flow equation corresponding to the assumed downstream boundary condition. Solutions obtained are assumed valid for channels IB, IC, IIB, and IIC. However, solutions for flow in channels ID and IID are discarded and then recomputed as channels IIIC and IIIB in segment III. Naturally, the algebraic sum of outflows from channels IB and IC at each time level constitutes the upstream inflow for channel ID (IIIC). Similarly, the sum of outflows from IIB and IIIC gives the upstream boundary condition for IID (IIB). Knowing the upstream inflows for channels IIIC and IIIB, computations are performed for segment III.

TABLE 1.—Properties of Example Open-Channel Network

Channel number (1)	Length, in feet (meters) (2)	Slope (3)	Width, in feet (meters) (4)	Manning <i>n</i> (5)
1	1968.5 (600)	0.0005	16.4 (5)	0.0138
2	1968.5 (600)	0.0005	16.4 (5)	0.0207
3	1968.5 (600)	0.0005	16.4 (5)	0.0207
4	1968.5 (600)	0.0005	16.4 (5)	0.0138
5	1968.5 (600)	0.0010	26.2 (8)	0.0141
6	1968.5 (600)	0.0010	32.8 (10)	0.0125

The single overlapping scheme just described may not be sufficiently accurate if the downstream backwater effect is serious and significant backwater propagates beyond one upstream channel. In this case a double overlapping scheme may be adopted.

COMPARISON WITH OTHER METHODS

In order to test the validity of the proposed diffusion wave model for simulation of flow in open-channel networks, comparisons with two other methods, namely, a dynamic wave and a kinematic wave models, have been made. The two models are briefly described as follows.

Implicit Nonlinear Dynamic Wave Model.—A four-point fully implicit scheme which is adopted in this study for dynamic-wave routing is a modified version of that proposed by Baltzer and Lai (2) to incorporate the simultaneous solutions

of the Saint-Venant and the junction equations. In this scheme, the finite difference quotients for a reach between flow sections *i* and *i* + 1 are written as

$$F_{i+0.5} \approx \frac{1}{2} (F_i^{j+1} + F_{i+1}^{j+1}) \quad \dots \dots \dots \quad (22)$$

$$\left(\frac{\partial F}{\partial x} \right)_{i+0.5} \approx \frac{1}{\Delta x} (F_{i+1}^{j+1} - F_i^{j+1}) \quad \dots \dots \dots \quad (23)$$

$$\left(\frac{\partial F}{\partial t} \right)_{i+0.5} \approx \frac{1}{2\Delta t} (F_{i+1}^{j+1} + F_i^{j+1} - F_{i+1}^j - F_i^j) \quad \dots \dots \dots \quad (24)$$

in which *F* = any reach function. The set of finite difference equations obtained

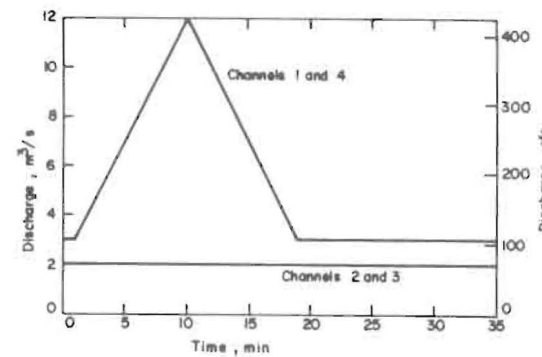


FIG. 6.—Upstream Inflow Hydrographs for Example I

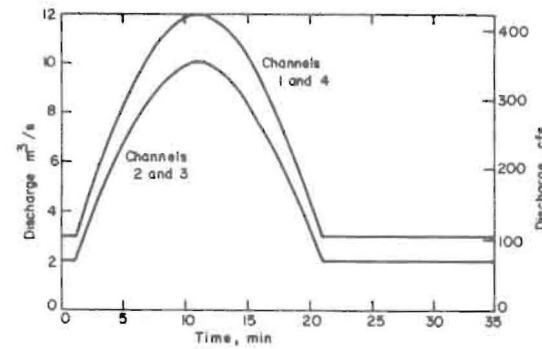


FIG. 7.—Upstream Inflow Hydrographs for Example II

by substituting Eqs. 22–24 into Eqs. 1 and 2 contains two unknowns, namely h_i^{j+1} and Q_i^{j+1} , for each flow section *i* along a channel. When a simple channel network composed of three junctions and seven branches as shown in Fig. 1 is considered, at each time step, the finite difference forms of Eqs. 1 and 2 provide $14(J - 1)$ nonlinear equations with $14J$ unknowns if the number

of flow sections selected along each channel is J . The additional 14 equations necessary for solving the problem are provided by four upstream boundary conditions for channels IB, IC, IIB, and IIC, one downstream boundary condition for channel IID, and nine junction equations, namely, Eqs. 6 and 7 applied to junctions I, II, and III. The solution is obtained by using the Newton iteration technique. The coefficient matrix obtained in each iteration cycle has a rank of $14J \times 14J$, and it is not banded. This makes the solution difficult and costly for small networks like that in Fig. 1 and unmanageable for larger systems.

Nonlinear Kinematic Wave Model.—In the kinematic-wave approximation, the inertia as well as pressure terms of the momentum equation (Eq. 2) are neglected and thus, the friction slope, S_f , is approximated by the bottom slope, S_b , of the channel (10). The downstream backwater effects of channels are neglected and each channel is treated individually. Computations start from the most upstream channels for which upstream boundary conditions are specified, and progress towards downstream channel by channel in a cascading manner, satisfying the flow continuity requirement at junctions. Along a channel reach with $S_f = S_b$, Eqs. 1 and 3 are combined to yield

$$\frac{\partial A}{\partial t} + \frac{\partial}{\partial x} \left(K A R^{2/3} \frac{S_b^{1/2}}{n} \right) = 0 \quad \dots \quad (25)$$

For a channel along which J flow sections are considered, by applying Eqs. 22, 23, and 24 to Eq. 25 and writing for $(J - 1)$ grids, together with an upstream boundary condition, a set of J nonlinear algebraic equations with J unknowns is obtained. The unknowns are h_i^{j+1} for $i = 1, 2, \dots, J$. This set of nonlinear equations are solved by using the Newton iteration method. The coefficient matrices involved are banded and thus, the solutions are obtained in a very efficient manner.

Comparison of Models.—Two hypothetical examples are presented here to demonstrate the validity and efficiency of the proposed diffusion wave model as compared to the other two models. The hypothetical network used in the examples consists of two junctions and six branches as shown in Fig. 5. All branches are assumed to be rectangular in cross section. The dimensions of the channels are listed in Table 1. The hypothetical floods that are routed through the network in the two examples are shown in Figs. 6 and 7, respectively. The initial condition for both examples is a steady flow condition corresponding to a discharge of $3 \text{ m}^3/\text{s}$ (106 cfs) in channels 1 and 4, $2 \text{ m}^3/\text{s}$ (71 cfs) in channels 2 and 3, $7 \text{ m}^3/\text{s}$ (247 cfs) in channel 5, and $10 \text{ m}^3/\text{s}$ (353 cfs) in channel 6. Downstream boundary condition at the exit of channel 6 is specified as a uniform flow equation assuming this channel is hydraulically long. A time increment of $\Delta t = 60 \text{ sec}$ is selected in both examples for all the three models. A constant reach length of $\Delta x = 60 \text{ m}$ (196.9 ft) is adopted for the diffusion and dynamic-wave models. The reach length is reduced to $\Delta x = 30 \text{ m}$ (98.4 ft) in the kinematic-wave model since numerical convergence could not be achieved with $\Delta x = 60 \text{ m}$ (196.9 ft).

The computed discharge hydrographs using the three models are shown in Figs. 8 and 9, respectively, for Examples I and II. As can be observed from these figures, the results of the proposed diffusion-wave model are in good agreement with those of the dynamic wave model. Conversely, the kinematic

wave solutions are not as reliable. The outflow hydrographs computed for channels 2 and 3 in Example I and shown in Fig. 8(b) clearly demonstrate the downstream backwater effects. In Example I, a constant upstream inflow of $2 \text{ m}^3/\text{s}$ (71 cfs) equal to the base flow rate is adopted for channels 2 and 3 as shown in Fig. 6. Thus, a steady flow condition would prevail in both channels 2 and 3 if the time variant backwater effects of the other channels in the network did not exist. Indeed, the kinematic wave method which ignores the backwater effects from downstream predicts a steady flow in these two branches as shown

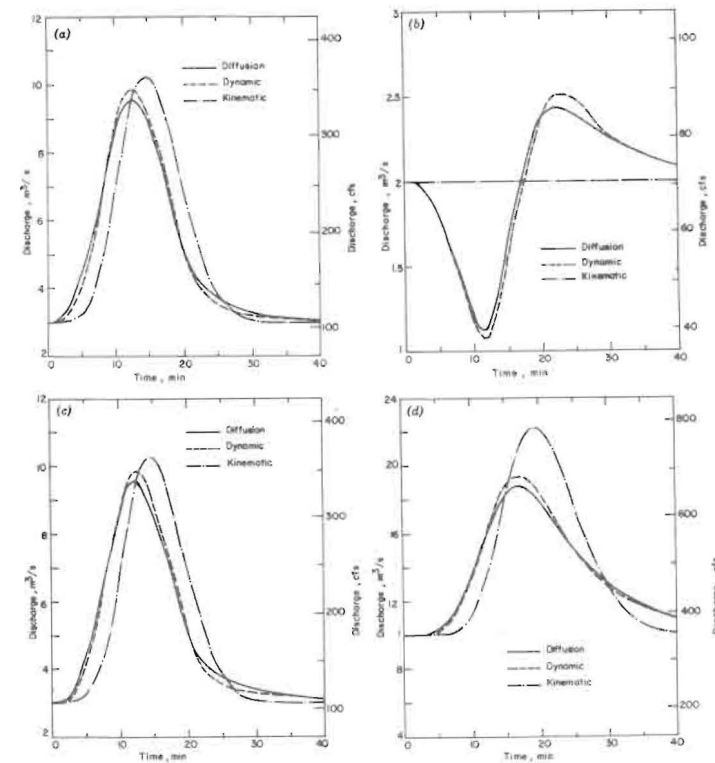


FIG. 8.—Comparison of Results of Example I: (a) Channel 1; (b) Channels 2 and 3; (c) Channel 4; and (d) Channel 6

in Fig. 8(b). However, in actuality, the flood wave travelling through channel 1 raises the water surface at the junction where branches 1, 2, and 3 join. This decreases the hydraulic gradient in channels 2 and 3 causing discharges lower than the constant upstream inflow and base flow rate. Naturally, from continuity requirements, the channel storage is increased during the period of low discharges. As the downstream backwater recedes with time, the excess water is released from the channel storage, and discharges higher than the constant inflow rate occur until steady state condition is again reached asymptotically. As shown in Fig. 8(b), this phenomena is satisfactorily simulated by both the

dynamic wave and proposed diffusion wave models but ignored completely in the kinematic wave model.

The computations for the two examples presented here was performed on an IBM 370/145 computer at the Middle East Technical University. For each one of the examples, the execution time was approx 90 sec, 150 sec, and 480 sec, respectively, for the diffusion, kinematic, and dynamic wave models. These values are presented merely as a reference. The noticeably different execution times for the kinematic and the diffusion wave models are partly due to a smaller computation grid adopted in the former, and partly due to faster

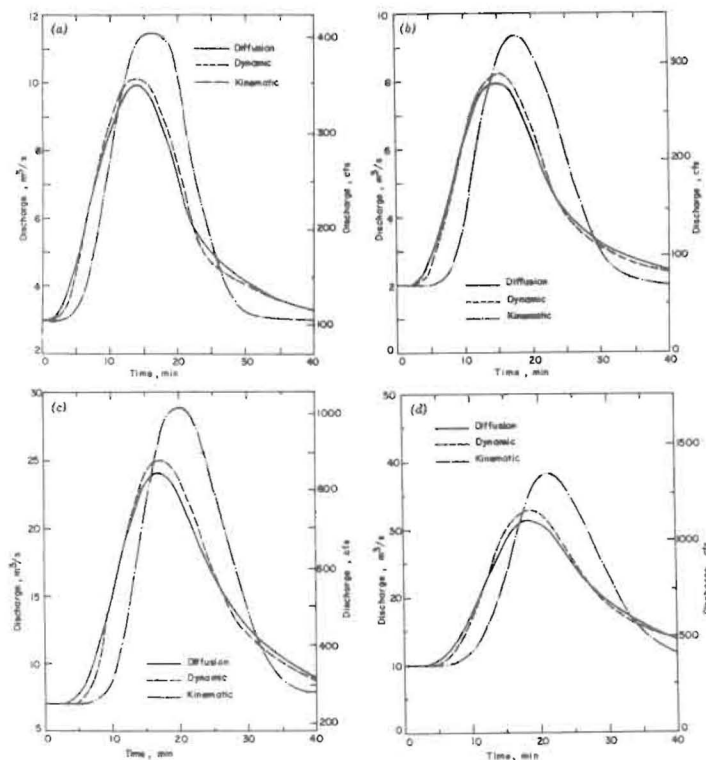


FIG. 9.—Comparison of Results of Example II: (a) Channel 1; (b) Channels 2 and 3; (c) Channel 5; and (d) Channel 6

convergence of numerical results in the latter model. The difference in computer execution times for these two models is smaller for other examples (not reported here) having identical grid sizes and numerical schemes which show consistently shorter execution time for the proposed diffusion wave model than the nonlinear kinematic wave model. The difference in the execution times for the diffusion and the dynamic wave models arises from faster convergence of the former and the difference in the structures of the two models and is expected to increase exponentially with increasing size of the network considered.

CONCLUSIONS

A nonlinear diffusion wave model for flood routing in dendritic-type open-channel networks is developed and presented in this study. Comparison of this model with dynamic wave and nonlinear kinematic wave models leads to the following conclusions:

1. The proposed diffusion-wave model can satisfactorily simulate the mutual backwater effects of channels joining at a junction.
2. The proposed model is nearly as accurate as the dynamic wave model which may be classified among the most sophisticated one-dimensional routing techniques available in the literature.
3. The proposed model is faster and cheaper in computation than a kinematic wave model which may be considered as one of the simplest hydraulic routing models known.

APPENDIX I.—REFERENCES

1. Akan, A. O., and Yen, B. C., "A Nonlinear Diffusion-Wave Model for Unsteady Open-channel Flow," *Proceedings of the 17th Congress, International Association for Hydraulic Research*, Vol. 2, Aug., 1977, pp. 181-190.
2. Baltzer, R. A., and Lai, C., "Computer Simulation of Unsteady Flows in Waterways," *Journal of the Hydraulics Division, ASCE*, Vol. 94, No. HY4, Proc. Paper 6048, July, 1968, pp. 1083-1117.
3. Bowers, C. E., Harris, G. S., and Pabst, A. F., "The Real-Time Computation of Runoff and Storm Flow in the Minneapolis-St. Paul Interceptor Sewers," *Memo. M-118*, St. Anthony Falls Hydraulics Laboratory, University of Minnesota, Dec., 1968.
4. Dronkers, J. J., *Tidal Hydraulics*, North-Holland Publishing Co., Amsterdam, The Netherlands, 1964, pp. 203-204.
5. Ponce, V. M., Li, R.-M., and Simons, D. B., "Applicability of Kinematic and Diffusion Models," *Journal of the Hydraulics Division, ASCE*, Vol. 104, No. HY3, Proc. Paper 13635, Mar., 1978, pp. 353-360.
6. Schaake, J. C., Jr., "Synthesis of the Inlet Hydrograph," *Storm Drainage Research Project Technology Report 3*, Johns Hopkins Univ., Baltimore, Md., June, 1965.
7. Sevük, A. S., "Unsteady Flow in Sewer Network," thesis presented to the University of Illinois at Urbana-Champaign, at Urbana, Ill., in 1973, in partial fulfillment of the requirements for the degree of Doctor of Philosophy.
8. Sevük, A. S., and Yen, B. C., "Comparison of Four Approaches in Routing Flood Wave through Junction," *Proceeding of the 15-th Congress, International Association for Hydraulic Research*, Vol. 5, Sept., 1973, pp. 169-172.
9. Yen, B. C., "Further Study on Open-Channel Flow Equations," *Sonderforschungsbereich 80 Publication No. SFB 80/T/49*, University of Karlsruhe, Karlsruhe, West Germany, Apr., 1975.
10. Yen, B. C., "Unsteady Flow Mathematical Modeling Techniques," *Modeling of Rivers*, H. W. Shen, ed., Chapter 13, Wiley-Interscience, Inc., New York, N.Y., 1979.
11. Yen, B. C., and Akan, A. O., "Flood Routing Through River Junctions," *Rivers '76*, Vol. I, ASCE, 1976, pp. 212-231.

APPENDIX II.—NOTATION

The following symbols are used in this paper:

- A* = flow cross-sectional area;
B = incoming channel;

S(200)
Am 81 hy
V.107
No. HY6

TECHNICAL PAPERS

Original papers should be submitted in triplicate to the Manager of Technical and Professional Publications, ASCE, 345 East 47th Street, New York, N.Y. 10017. Authors must indicate the Technical Division or Council, Technical Committee, Subcommittee, and Task Committee (if any) to which the paper should be referred. Those who are planning to submit material will expedite the review and publication procedures by complying with the following basic requirements:

1. Titles must have a length not exceeding 50 characters and spaces.
2. The manuscript (an original ribbon copy and two duplicate copies) should be double-spaced on one side of 8-1/2-in. (220-mm) by 11-in. (280-mm) paper. Three copies of all figures and tables must be included.
3. Generally, the maximum length of a paper is 10,000 word-equivalents. As an approximation, each full manuscript page of text, tables or figures is the equivalent of 300 words. If a particular subject cannot be adequately presented within the 10,000-word limit, the paper should be accompanied by a rationale for the overlength. This will permit rapid review and approval by the Division or Council Publications and Executive Committees and the Society's Committee on Publications. Valuable contributions to the Society's publications are not intended to be discouraged by this procedure.
4. The author's full name, Society membership grade, and a footnote stating present employment must appear on the first page of the paper. Authors need not be Society members.
5. All mathematics must be typewritten and special symbols must be identified properly. The letter symbols used should be defined where they first appear, in figures, tables, or text, and arranged alphabetically in an appendix at the end of the paper titled Appendix.—Notation.
6. Standard definitions and symbols should be used. Reference should be made to the lists published by the American National Standards Institute and to the *Authors' Guide to the Publications of ASCE*.
7. Figures should be drawn in black ink, at a size that, with a 50% reduction, would have a published width in the *Journals* of from 3 in. (76 mm) to 4-1/2 in. (110 mm). The lettering must be legible at the reduced size. Photographs should be submitted as glossy prints. Explanations and descriptions must be placed in text rather than within the figure.
8. Tables should be typed (an original ribbon copy and two duplicates) on one side of 8-1/2-in. (220-mm) by 11-in. (280-mm) paper. An explanation of each table must appear in the text.
9. References cited in text should be arranged in alphabetical order in an appendix at the end of the paper, or preceding the Appendix.—Notation, as an Appendix.—References.
10. A list of key words and an information retrieval abstract of 175 words should be provided with each paper.
11. A summary of approximately 40 words must accompany the paper.
12. A set of conclusions must end the paper.
13. Dual units, i.e., U.S. Customary followed by SI (International System) units in parentheses, should be used throughout the paper.
14. A practical applications section should be included also, if appropriate.

VOL. 107 NO. HY6, JUNE 1981

JOURNAL OF THE HYDRAULICS DIVISION

PROCEEDINGS OF
THE AMERICAN SOCIETY
OF CIVIL ENGINEERS

